Novel Red Phosphorescent Polymers Bearing Both Ambipolar and Functionalized Ir^{III} Phosphorescent Moieties for Highly Efficient Organic Light-Emitting Diodes

Jiang Zhao, Meng Lian, Yue Yu, Xiaogang Yan, Xianbin Xu, Xiaolong Yang, Guijiang Zhou,* Zhaoxin Wu*

A series of novel red phosphorescent polymers is successfully developed through Suzuki cross-coupling among ambipolar units, functionalized Ir^{III} phosphorescent blocks, and fluorene-based silane moieties. The photophysical and electrochemical investigations indicate not only highly efficient energy-transfer from the organic segments to the phosphorescent units in the polymer backbone but also the ambipolar character of the copolymers. Benefiting from all these merits, the phosphorescent polymers can furnish organic light-emitting diodes (OLEDs) with exceptional high electroluminescent (EL) efficiencies with a current efficiency (η_L) of 8.31 cd A^{-1}, external quantum efficiency (η_{ext}) of 16.07%, and power efficiency (η_P) of 2.95 lm W^{-1}, representing the state-of-the-art electroluminescent performances ever achieved by red phosphorescent polymers. This work here might represent a new pathway to design and synthesize highly efficient phosphorescent polymers.

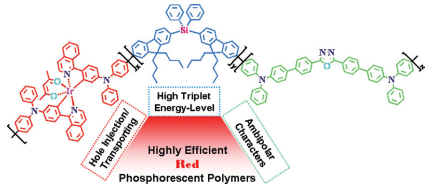

1. Introduction

Due to their advantages in making devices with low cost, light weight, flexibility, and at large scale by using cheap solution processing approaches, such as spin-coating, ink-jet, and roll-to-roll, etc.,[1–4] emissive polymers have drawn substantial research interests from both academic and industrial communities for the use in organic light-emitting diodes (OLEDs), which have been regarded as the most competitive candidates for both future displays and solid lighting sources with energy-saving features.[3,5] Unfortunately, compared with the devices made from small molecular emitters through vacuum-deposition, solution-processed OLEDs with polymers as emitters typically exhibit much lower electroluminescent (EL) efficiencies. This situation has set a big obstacle for polymeric emitters considering their application in practical displays and lighting sources. Hence, concerned researchers continuously devote their efforts to find high-performance polymeric emitters to fabricate efficient OLEDs with cheap solution approaches. Introducing phosphorescent (triplet) blocks to the polymeric backbone to develop phosphorescent polymers might represent the most successful

J. Zhao, M. Lian, X. Yan, X. Xu, X. Yang, Prof. G. Zhou
MOE Key Laboratory for Nonequilibrium Synthesis and Modulation of Condensed Matter, State Key Laboratory for Mechanical Behavior of Materials, Institute of Chemistry for New Energy Material, Department of Chemistry, Faculty of Science, Xi'an Jiaotong University, Xi'an 710049, China
E-mail: zhougj@mail.xjtu.edu.cn
Y. Yu, Prof. Z. Wu
Key Laboratory of Photonics Technology for Information, School of Electronic and Information Engineering, Xi'an Jiaotong University, Xi'an 710049, China
E-mail: zhaoxinwu@mail.xjtu.edu.cn

DOI: 10.1002/marc.201400490

strategy to enhance the EL efficiencies of polymer light-emitting diodes (PLEDs), since the phosphorescent units can harness both singlet and triplet excitons for the EL process.[3c,d,6]

Until now, a large number of phosphorescent polymers has been developed by introducing phosphorescent units, typically 2-phenylpyridine-type (ppy-type) iridium(III) complexes, to either the main chain[7] or side chain.[6a,8] In order to relieve the undesired back energy transfer from the phosphorescent moieties to the nonemissive triplet state of the conjugated polymer backbones, phosphorescent polymers with nonconjugated backbones have also been developed.[9] With the aim to solve the charge carrier injection/transporting problems, researchers have further introduced novel phosphorescent polymers with functional groups showing charge carrier injection/transporting capacity, such as triphenylamine, carbazole, and oxadiazole, etc.[10] Additionally, phosphorescent polymer with phosphine oxide ether backbones are developed to furnish high EL efficiencies.[11] Through these advanced strategies, green phosphorescent polymers can achieve an EL efficiency of 33.9 cd A^{-1}[12], and the highly efficient blue analogs can show attractive efficiencies of 28.1 cd A^{-1}.[9b] Despite these exciting achievements, most of the phosphorescent polymers developed up to now still show low EL efficiencies of less than 10 cd A^{-1}. Compared with their green and blue counterparts, red phosphorescent polymers even show poor EL performances with an EL efficiency typically less than 5 cd A^{-1}.[3c] As one of the three primary colors, red color is indispensible for high-quality display and lighting purpose. Hence, developing highly-efficiency red phosphorescent polymers will definitely represent a very tough task needed to be fulfilled urgently, considering the practical application of OLEDs.

Recently, developing functionalized phosphorescent emitters with carrier injection/transporting feature has been shown as very important strategy to enhance the EL efficiencies of the concerned phosphorescent OLEDs (PHOLEDs).[13] In addition, the ambipolar host materials can also effectively enhance the EL performances of PHOLEDs by expanding the combination zone and achieving more balanced injection/transporting for both kinds of charge carriers.[14] Obviously, these new strategies should provide valuable inspirations for design of novel highly efficient red phosphorescent polymers. Bearing this in mind, we have designed and prepared highly efficient red phosphorescent polymers with both triphenylaime-functionalized phosphorescent blocks and ambipolar triphenylamine-oxadiazole hybrid units. Furthermore, fluorene-based silane blocks have also been employed to increase their triplet energy level of the backbones of these new polymers to relieve the trouble of back energy transfer and to furnish high EL efficiencies.

2. Experimental Section

2.1. General Information

All reactions were carried out under nitrogen atmosphere. The solvents were purified by standard methods under dry nitrogen before use. All commercially available reagents were used as received unless otherwise stated. The reactions were monitored by thin-layer chromatography (TLC) with Merck precoated aluminum plates. Flash column chromatography and preparative TLC were carried out using silica gel. All Suzuki copolymerization reactions were carried out with the Schlenk techniques in nitrogen atmosphere.

2.2. Analytical Techniques

^{1}H NMR and ^{13}C NMR spectra were measured in $CDCl_3$ or DMSO-d_6 with a Bruker AXS 400 MHz spectrometer with the chemical shifts quoted relative to tetramethylsiliane (TMS). Fast atom bombardment (FAB) mass spectra were recorded on a Finnigan MAT SSQ710 system. UV–Vis spectra were recorded with a Shimadzu UV-2250 spectrophotometer. The photoluminescent (PL) properties of the copolymers were measured with an Edinburgh Instruments FLS920 fluorescence spectrophotometer. The lifetimes for the excited states were measured by a single photon counting spectrometer from Edinburgh Instruments FLS920 with a 400 nm picosecond LED lamp as the excitation source. Differential scanning calorimetry (DSC) was performed with a NETZSCH DSC 200 PC unit under a nitrogen flow at a heating rate of 10 °C min^{-1}. Thermogravimetric analysis (TGA) was conducted with a NETZSCH STA 409C instrument under nitrogen with a heating rate of 20 °C min^{-1}. The molecular weights of the copolymers were determined by Waters 2695 GPC in THF. The weights were estimated by using a calibration curve of polystyrene standards. Cyclic voltammetry (CV) measurement for the sample solution was performed on Princeton Applied Research model 2273A potentiostat with a glassy carbon working electrode, a platinum counter electrode, and a platinum-wire reference electrode at a scan rate of 100 mV s^{-1}. The solvent was deoxygenated dichloromethane, and the supporting electrolyte was 0.1 M [nBu$_4$N][BF_4]. Ferrocene (Fc) was added as an internal calibrant for the measurement, and all potentials reported were quoted with reference to the Fc/Fc^+ couple. The polymer films on quartz substrate were obtained by spin-coating their chlorobenzene solution (ca. 20 mg mL^{-1}) and their thickness was determined by Nanoview SE MF-1000 Ellipsometer. The triplet energy levels have been obtained by the 77 K PL spectra, which were obtained by dipping the degassed sample CH_2Cl_2 solution in thin quartz tube into liquid nitrogen Dewar and recorded the PL spectra after standing 5 min. In order to avoid the interference from the strong singlet emission, the 77 K PL spectrum for the pure organic polymer was obtained with highly dilute solution.

2.3. Synthesis

The preparation details of the key monomers IrM, BP-Br, and FlSi-B were presented in Scheme S1 (Supporting Information).

2.3.1. P-R-1

Under N_2 atmosphere, Ir-M (2.0 mg, 0.0017 mmol), BP-Br (42.2 mg, 0.0488 mmol), FlSi-B (49.9 mg, 0.0505 mmol), Na_2CO_3 (0.13 g, 1.23 mmol), and $Pd(PPh_3)_4$ (9.24 mg, 0.008 mmol) were mixed in a solvent mixture of degassed toluene/THF/H_2O(5.0 mL/5.0 mL/1.25 mL). The mixture was vigorously stirred for 48 h at 100 °C. The reaction mixture was then stirred at 100 °C for 12 h after adding phenylboronic acid (3.0 mg, 0.025 mmol), and then stirred at 100 °C for a further 12 h after adding bromobenzene (4.0 mg, 0.025 mmol). After adding water (20 mL), the mixture was extracted with CH_2Cl_2 (3 × 25 mL) and the organic phase was dried over anhydrous Na_2SO_4. Then, the solvent was removed and the residue was redissolved in CH_2Cl_2 and purified by 0.45 μm PTFE syringe filter. After concentration, the copolymer was purified by precipitation twice in methanol and washed with acetone in a Soxhlet apparatus for 72 h, and dried under vacuum. It was obtained as light orange solid (yield: 70%). ^{1}H NMR (400 MHz, $CDCl_3$, δ, ppm): 8.20 (d), 7.77–7.05 (m), 1.97–1.90 (m), 1.10–1.08 (m), 0.72–0.69 (m); Gel permeation chromatography (GPC): number-average molecular weight (M_n) = 3.2×10^4 g mol^{-1}, polydispersity index (PDI) = 1.9 (against polystyrene standards).

2.3.2. P-R-2

It was prepared from Ir-M (4.0 mg, 0.0034 mmol), BP-Br (40.7 mg, 0.0471 mmol), FlSi-B (49.9 mg, 0.0505 mmol), Na_2CO_3 (0.13 g, 1.23 mmol), and $Pd(PPh_3)_4$ (9.24 mg, 0.008 mmol), following the same procedure as for P-R-1. The copolymer was obtained as orange solid (yield: 80%). ^{1}H NMR (400 MHz, $CDCl_3$, δ, ppm): 8.21 (d), 7.79–7.08 (m), 1.99–1.95 (m), 1.11–1.06 (m), 0.73–0.69 (m); GPC: $M_n = 3.3 \times 10^4$ g mol^{-1}, PDI = 1.8 (against polystyrene standards).

2.3.3. P-R-3

It was prepared from Ir-M (6.0 mg, 0.0050 mmol), BP-Br (39.3 mg, 0.0455 mmol), FlSi-B (49.9 mg, 0.0505 mmol), Na_2CO_3 (0.13 g, 1.23 mmol), and $Pd(PPh_3)_4$ (9.24 mg, 0.008 mmol), following the same procedure as for P-R-1. The copolymer was obtained as orange solid (yield: 84%). ^{1}H NMR (400 MHz, $CDCl_3$, δ, ppm): 8.20 (d), 7.80–6.99 (m), 5.21 (s), 1.97–1.95 (m), 1.80 (s), 1.09–1.06 (m), 0.72–0.67 (m); GPC: $M_n = 3.1 \times 10^4$ g mol^{-1}, PDI = 2.0 (against polystyrene standards).

2.3.4. P-R-4

It was prepared from Ir-M (8.0 mg, 0.0067 mmol), BP-Br (37.8 mg, 0.0438 mmol), FlSi-B (50 mg, 0.0505 mmol), Na_2CO_3 (0.13 g, 1.23 mmol), and $Pd(PPh_3)_4$ (9.24 mg, 0.008 mmol), following the same procedure as for P-R-1. The copolymer was obtained as orange solid (yield: 82%). ^{1}H NMR (400 MHz, $CDCl_3$, δ, ppm): 8.20 (d), 7.75–6.99 (m), 5.21 (s), 1.97–1.93 (m), 1.80 (s), 1.08–1.05 (m), 0.74–0.64 (m); GPC: $M_n = 3.4 \times 10^4$ g mol^{-1}, PDI = 1.9 (against polystyrene standards).

2.3.5. P-Org

Under N_2 atmosphere, BP-Br (43.7 mg, 0.0506 mmol), FlSi-B (50 mg, 0.0506 mmol), Na_2CO_3 (0.13 g, 1.23 mmol), and $Pd(PPh_3)_4$ (9.24 mg, 0.008 mmol) were mixed in a solvent mixture of degassed toluene/THF/H_2O (5.0 mL/5.0 mL/1.25 mL). The mixture was vigorously stirred for 48 h at 100 °C. The reaction mixture was then stirred at 100 °C for 12 h after adding phenylboronic acid (3.0 mg, 0.025 mmol), and then stirred at 100 °C for a further 12 h after adding bromobenzene (4.0 mg, 0.025 mmol). After adding water (20 mL), the mixture was extracted with CH_2Cl_2 (3 × 25 mL) and the organic phase was dried over anhydrous Na_2SO_4. Then the solvent was removed and the residue was redissolved in CH_2Cl_2 and purified by 0.45 μm PTFE syringe filter. After concentration, the copolymer was purified by precipitation twice in methanol and washed with acetone in a Soxhlet apparatus for 72 h, and dried under vacuum. It was obtained as pale yellow solid (Yield: 87%). ^{1}H NMR (400 MHz, $CDCl_3$, δ, ppm): 8.21 (d), 7.76–7.01 (m), 1.98–1.94 (m), 1.11–1.09 (m), 0.75–0.69 (m); Gel permeation chromatography (GPC): number-average molecular weight (M_n) = 3.2×10^4 g mol^{-1}, polydispersity index (PDI) = 2.3 (against polystyrene standards).

2.4. OLED Fabrication and Measurements

The precleaned ITO glass substrates were treated with ozone for 20 min. Then, the PEDOT:PSS was deposited on the surface of ITO glass by the spin-coating method to form a 40 nm thick hole-injection layer after being cured at 120 °C for 30 min in the air. The emitting layer (40 nm) was obtained by spin-coating a chlorobenzene solution of each corresponding phosphorescent polymer. The ITO glass was dried in a vacuum oven at 50 °C for 15 min and it was transferred to the deposition system for organic and metal deposition. TPBi (40 nm), LiF (1 nm), and Al cathode (100 nm) were successively evaporated at a base pressure less than 10^{-6} Torr. The EL spectra and CIE coordinates were measured with a PR650 spectra colorimeter. The *L–V–J* curves of the devices were recorded by a Keithley 2400/2000 source meter and the luminance was measured using a PR650 SpectraScan spectrometer. All the experiments and measurements were carried out under ambient conditions.

3. Results and Discussion

3.1. Synthesis and Characterization

All the monomers Ir-M, BP-Br, and FlSi-B required to construct phosphorescent polymers have been prepared by the procedures shown in Scheme S1 (Supporting Information). The phosphorescent monomer Ir-M was prepared according to the established two-step strategy by the cyclometalation of $IrCl_3 \cdot nH_2O$ with the corresponding organic ligands, followed by coordination of the acetylacetone (acac) anion in the presence of [Tl(acac)] under very mild condition. In Ir-M, functional group of triphenylamine was introduced to afford hole- injection/transporting (HI/HT) ability. The ambipolar monomer BP-Br has been prepared by the bromination of BP with NBS. The ambipolar property of BP-Br is afforded by both the 1,3,4-oxadiazole unit with electron injection/transporting (EI/ET)

property and triphenylamine moiety with HI/HT feature. The FlSi-B was synthesized by the cross-coupling between FlSi-Br and bis(pinacolato)diboron under base condition with Pd(dppf)Cl_2 as catalyst (Scheme S1, Supporting Information). Due to its high triplet energy level, fluorene-based silane block in FlSi-B has been designed with the aim to block undesired back energy transfer process.

The two pinacol ester groups can afford FlSi-B the ability of copolymerization with Ir-M and BP-Br to form the designed phosphorescent polymers, which were prepared by the procedure shown in Scheme 1. The feed ratio of the red phosphorescent monomer Ir-M was set 1.68 to 6.63 mol%, the corresponding weight percentage ca. 2.0, 4.0, 6.0, and 8.0 wt%. According to the feed ratios of Ir-M, FlSi-B, and BP-Br, the obtained copolymers are named P-R-1 (1.68:50:48.32), P-R-2 (3.37:50:46.63), P-R-3 (4.95:50:45.05), and P-R-4 (6.63:50:43.37), respectively (Scheme 1).

In the ^{1}H NMR spectra of the polymers, the resonance peaks with δ at ca. 1.99–1.95, 1.10–1.05, and 0.74–0.64 ppm can be assigned to the butyl group of the fluorene-based blocks. The proton signal with δ at 8.20 ppm should be induced by the ambipolar segment, comparing

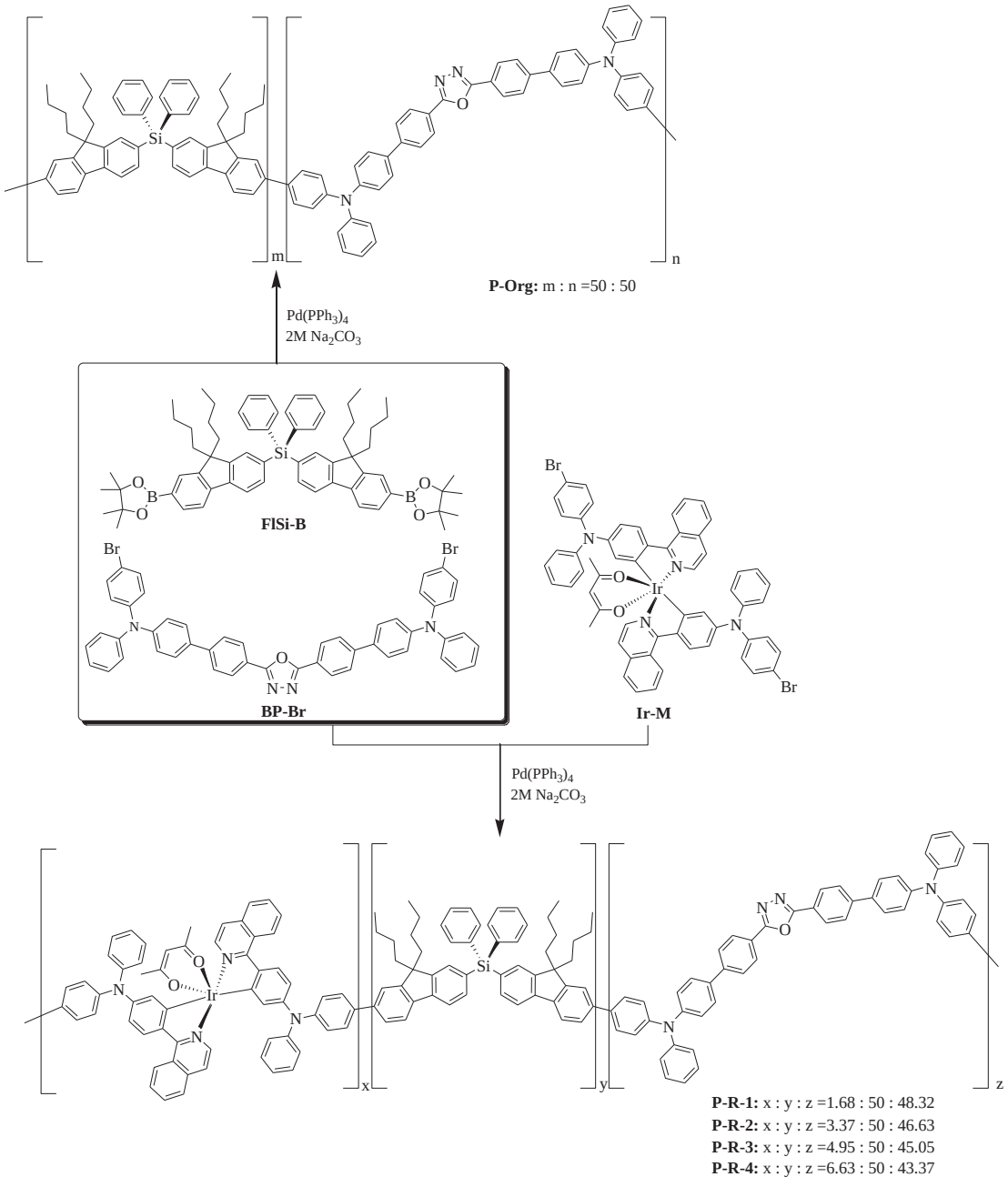

Scheme 1. Synthetic scheme for red phosphorescent polymers and the model polymer P-Org.

with that of BP-Br (see Supporting Information). Owing to the low content of the phosphorescent moieties, the associated ^1H NMR signals cannot be detected obviously. However, very weak resonance signal with δ at ca. 5.21 and 1.80 ppm can still be detected for P-R-3 and P-R-4. These are the characteristic proton signals of the acac anion in the Ir^{III} phosphorescent blocks. All these spectral data have properly indicated that all the building blocks have been copolymerized together successfully. These phosphorescent polymers are readily soluble in common organic solvents, such as $CHCl_3$, CH_2Cl_2, and THF, *etc.* Taking polystyrene as standards, the number- average molecular weights (M_n) of the copolymers range from 3.1×10^4 to 3.4×10^4 with polydispersity indices (PDIs) ca. 2.0.

With the aim to investigate the photophysical and electrochemical properties of the red phosphorescent polymers, the model pure organic polymers P-Org was also obtained through the Suzuki cross-coupling between BP-Br and FlSi-B (Scheme 1).

3.2. Thermal, Photophysical Properties, and Electrochemistry

The thermal behaviors of the phosphorescent copolymers have been investigated by TGA and DSC under nitrogen atmosphere. The TGA results indicate their thermal stability with the 5% weight-reduction temperature ($\Delta T_{5\%}$) at ca. 410 °C (Table S1, Supporting Information). The DSC traces of the copolymers have revealed their high glass-transition temperatures (T_g) ca. 125 °C (Table S1, Supporting Information). The good thermal properties will benefit their application in the field of OLEDs.

In their UV–Vis spectra (Figure 1a), the main absorption bands of the copolymers are located before ca. 450 nm. It can be safely assigned to the π–π^* transition from both the aromatic silane and ambipolar units. The contribution from the π–π^* transition of organic ligands from Ir^{III} phosphorescent units should be inessential due to their low content in the copolymers. However, for the copolymers with higher Ir^{III} phosphorescent chromophor content, such as P-R-3 and P-R-4, inconspicuous absorption bands with very low intensity can be observed, which can be assigned to the metal-to-ligand charge transfer states for both singlet (^{1}MLCT) and triplet (^{3}MLCT) from the phosphorescent units (Figure 1a and Table S1, Supporting Information).

The PL spectra for the phosphorescent copolymers are also measured in both solution and film state (Figure S1, Supporting Information and Figure 1b). The copolymer films deposited on the quartz substrate possess similar thickness of ca. 200 nm. In CH_2Cl_2 solution, all the copolymers exhibit emission band at ca. 490 nm (Figure S1 and Table S1, Supporting Information). Based on their nanosecond lifetime together with the PL spectrum of the

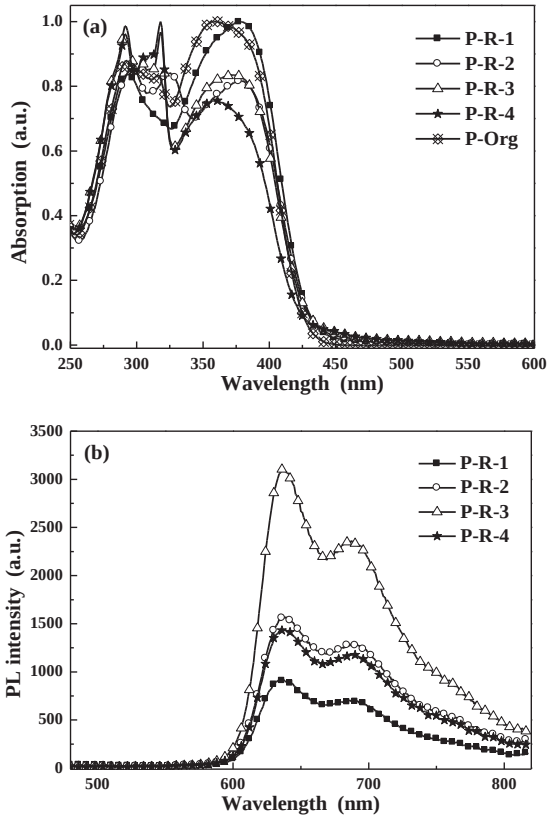

Figure 1. a) UV–Vis spectra of the phosphorescent polymers and the model polymer P-Org in CH_2Cl_2 at 298 K. b) Photoluminescence (PL) spectra for the neat films of the phosphorescent polymers.

polymer P-Org (Table S1 and Figure S1, Supporting Information), these emission bands should be induced by the pure organic segments in the phosphorescent copolymers. Differently, these copolymers can show intense red phosphorescent bands at ca. 637 nm in film state (Figure 1b and Table S1, Supporting Information). The phosphorescent emission bands of the copolymer films generally are enhanced with increasing of the content level of phosphorescent units (Figure 1b). However, the phosphorescent intensity shows substantial decreasing at high content of the Ir^{III} complex blocks (P-R-4) due to the quenching effect among the phosphorescent units (Figure 1b). For all the phosphorescent polymers, the high-energy emission band totally disappears (Figure 1b) due to the efficiency energy transfer from the pure organic segments to the phosphorescent units, which is typically shown in phosphorescent polymers. The photophysical properties of the organic segments formed between BP-Br and FlSi-B in the polymer backbones should be similar to those of P-Org due to the low content of the Ir^{III} monomers. The ratiocination has been confirmed by the great resemblance between their UV–vis, PL, and lifetime (Figure 1a, Figure S1, and Table S1, Supporting Information). Hence, the

photophysical property of P-Org can be safely employed to represent that of the organic segments in the red phosphorescent polymer backbones. According to the UV–Vis spectra of P-Org and Ir-M in Figure 2a, the 400 nm light can induce the excitation of organic segments in the phosphorescent polymers as well as the organic ligands of the Ir^{III} monomers. For P-R-1–P-R-4, energy level for the first singlet states (S_1') of their organic segments is higher than that for the first singlet states (S_1^R) of the organic ligands in Ir-M (Figure 2a). There should be cascade energy-transfer process from S_1' to S_1^R, then from S_1^R to $^1MLCT^R$ (singlet states of MLCT in Ir-M), which is converted via intersystem crossing (ISC) into emissive $^3MLCT^R$ (triplet states of MLCT in Ir-M) (Figure 2b) to induce phosphorescence signal in P-R-1–P-R-4 (Figure 1b). Another possible energy-transfer pathway can be from the first triplet states (T_1', ca. 2.23 eV) of their organic segments produced by the ISC via S_1' to $^3MLCT^R$ (ca. 1.96 eV) (Figure S2, Supporting Information), which can induce phosphorescence in P-R-1–P-R-4 as well (Figure 1b). However, different from the electric excitation, the T_1' will be formed in very low probability in photo excitation process. So, this pathway might give small contribution to the energy transfer involved in the phosphorescent copolymers. According to the energy-level involved, all the energy-transfer processes in P-R-1–P-R-4 are energy-favored down-hill procedure to guarantee their high efficiency (Figure 2b). Additionally, there is good overlap between the absorption spectrum of Ir-M and the PL spectrum of P-Org (Figure 2a), indicating the facilitation of the energy transfer from the organic segments to phosphorescent units in these red phosphorescent polymers. Hence, the highly efficient cascade energy-transfer process should greatly reduce chance for the decay of S_1' to the ground state (S_0). Hence, there is nearly no high-energy fluorescent emission bands associated with the transition of S_1' to S_0 in the phosphorescent polymer films (Figure 1b).

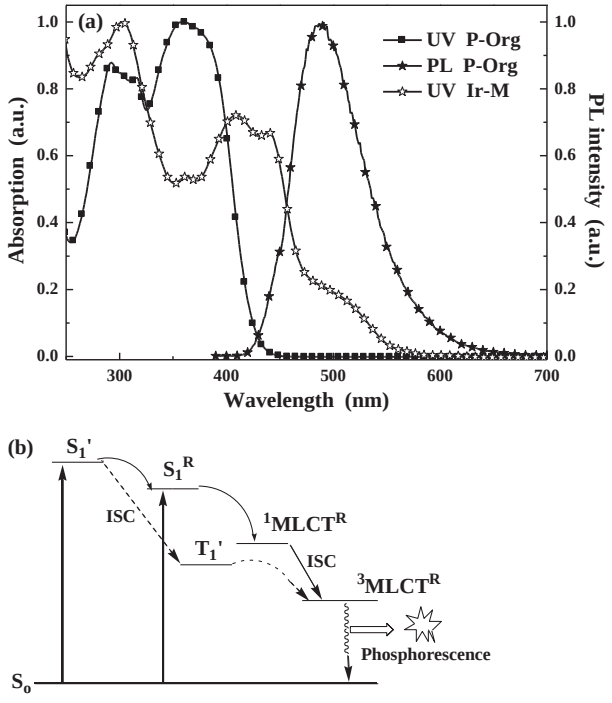

Figure 2. a) UV–Vis spectra of P-Org and Ir-M together with the PL spectrum of P-Org in CH_2Cl_2 at 298 K. b) Energy-transfer sketch involved in the red phosphorescent copolymers.

The electrochemical behavior of these phosphorescent polymers was characterized by the cyclic voltammetry (CV) measurements calibrated with ferrocene (Fc) as the internal standard under nitrogen atmosphere. All the phosphorescent polymers show a reversible oxidation process at ca. 0.5 V, ranging from 0.42 to 0.56 V (Table S2, Supporting Information). Similarly, these polymers also show alike reduction potential at ca. –2.5 V (Table S2, Supporting Information). With the aim to assign the oxidation and reduction processes, the CV data of P-Org are also obtained. The P-Org exhibits $E_{1/2}^{ox}$ at ca. 0.5 V and $E_{1/2}^{red}$ at ca. –2.50 V, which are very similar to those of the phosphorescent polymers. Based on electronic characters of the aromatic units involved in P-Org,[15] the CV waves should be assigned to the ambipolar units in the backbone of P-Org. All the obtained results indicate that the redox processes involved in the phosphorescent copolymers come from the ambipolar units as well. Due to its low content, the CV signal associated with the Ir^{III} phosphorescent units cannot be properly detected. Taking all the CV results into consideration, it can be concluded that introducing ambipolar moieties can effectively improving the injection ability for both kinds of charge carriers of the concerned phosphorescent copolymers, which should benefit the EL performance of the investigated copolymers.

3.3. Electroluminescent Devices

In order to evaluate the EL potential of these novel red phosphorescent polymers, the solution-processed PHOLEDs have be fabricated with the configuration of ITO/PEDOT:PSS (40 nm)/emission layer, EML (40 nm)/TPBi (40 nm)/LiF (1 nm)/Al (100 nm) (Figure S2, Supporting Information). The PEDOT:PSS layer was used as hole-injection layer (HIL). The 1,3,5-tris(1-phenyl-1*H*-benzo[*d*]-imidazol-2-yl)benzene (TPBi) layer plays the role of both hole-blocking and electron-transporting, while LiF acts as an electron-injection layer.

When a proper voltage is applied to the PHOLEDs, intense red electrophosphorescence at ca. 640 nm can be observed (Figure 3). For devices R1– R4 with P-R-1–P-R-4 as emitter (Figure S3, Supporting Information), they show red EL spectra representing a similar line-shape to that of the

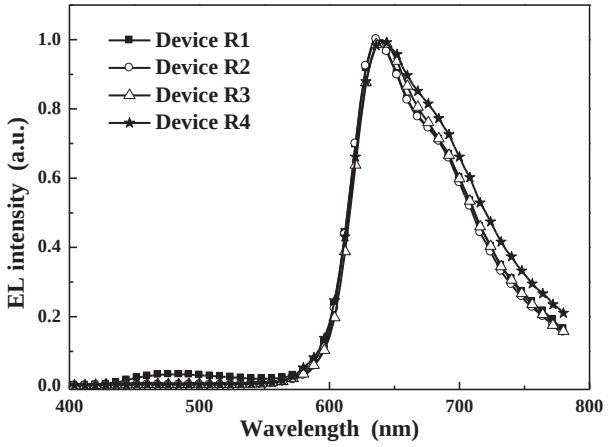

Figure 3. EL spectra for the solution-processed PHOLEDs at ca. 12 V.

corresponding polymers in the film state, indicating the origin of EL is from the phosphorescent units (Figure 1b). There is only very a weak EL band from organic segments in the polymer P-R-1 for device R1 due to the low level of the phosphorescent units, which cannot intake all the energy transferred from the organic segments in the polymer (Figure 3). In other devices, there should be complete energy-transfer processes.

The current-density-voltage-luminance (*J-V-L*) curves for the PHOLEDs are shown in Figure 4a and Figure S4 (Supporting Information). The corresponding EL data are summarized in Table S3 (Supporting Information). From device R1 to R4, the turn-on voltages decrease from 8.1 to 4.6 V (Table S3, Supporting Information), which might benefit from the excellent HI/HT ability associated with the functionalized phosphorescent Ir^{III} blocks. From the CV results (Table S2, Supporting Information), the functionalized phosphorescent blocks display much lower first oxidation potential of $E_{1/2}{}^{ox}$ at ca. 0.31 V due to both the coordination of triphenylamine with Ir(III) center[16] and its inherent electron-rich character. Obviously, increasing the content of the phosphorescent blocks in the polymer backbone should benefit the HI/HT process to the emission layer of the OLEDs, which will definitely benefit the lowing of turn-on voltages. This result also indicates the advantages of introducing functionalized phosphorescent units to the copolymer backbone. Among all the red solution-processed PHOLEDs, device **R3** can show the best EL performances with peak luminance (L_{max}) of 5402 cd m^{-2} at 18.9 V, current efficiency (η_L) of 8.31 cd A^{-1}, external quantum efficiency (η_{ext}) of 16.07% and power efficiency (η_P) of 2.95 lm W^{-1} (Figure 4b and Table S3, Supporting Information). Besides, device R2 can also show attractive EL potentials. Device R2 can exhibit peak EL performance with L_{max} of 6334 cd m^{-2} at 15.9 V, η_L of 4.90 cd A^{-1}, η_{ext} of 9.12% and η_P of 1.85 lm W^{-1}. Furthermore, device R4 furnishes L_{max} of 2456 cd m^{-2} at 21.3 V, η_L of 4.46 cd A^{-1},

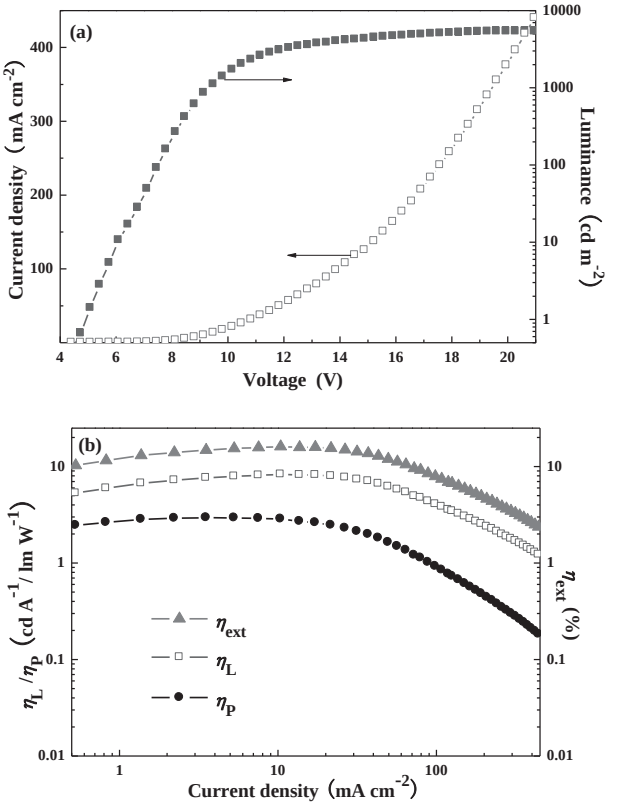

Figure 4. a) Current-density-voltage–luminance (*J-V-L*) curves for device R3. b) Relationship between EL efficiencies and current density for device R3.

η_{ext} of 8.76%, and η_P of 2.39 lm W^{-1}, respectively (Figure S5 and Table S3, Supporting Information). However, device R4 suffers more serious efficiency roll-off, which can be ascribed to the triplet-triplet annihilation effect induced by the high content of the phosphorescent units in P-R-4 as aforementioned (Figure 1b). Clearly, these exceptional high EL performances associated with the red phosphorescent polymers should benefit from the judicious molecular design notion to fulfill structural optimization. Until now, many high-performance red phosphorescent polymers have been reported in the literature. The red phosphorescent polymers with carbazole-*alt*-fluorene backbone and quinoline-based Ir^{III} units in the side chain can achieve EL efficiencies of 4.0 cd A^{-1} and of 4.9%.[6a] The phosphorescent polymer with red-emitting isoquinoline-based Ir^{III} complex embedded in the fluorene-*alt*-spirobifluorene backbone can show high η_{ext} of 3.21%.[17] With the red phosphorescent benzothiophene-based Ir^{III} complex in the side chain, the phosphorescent polymers with fluorene backbone can achieve η_{ext} of 2.0%.[8c] Through attaching both functional groups and the red-emitting benzothiophene-based Ir^{III} complex to the side chains, the phosphorescent polymer with nonconjugated backbone has been developed to show η_{ext} of 5.1% and η_P of

3.3 lm W^{-1}.[9a] Compared with these outstanding reported results about the red phosphorescent polymers, the concerned polymers definitely can show very attractive EL performances. The concerned results should provide valuable guidance for design and synthesis of highly efficient phosphorescent polymers.

4. Conclusion

Based on the functionalization idea, novel phosphorescent polymers have been successfully prepared with the aim to provide highly efficient polymeric red emitters. Through combination of functionalized Ir^{III} phosphorescent units with HI/HT ability, ambipolar blocks, and flourene-based silane moieties with high triplet energy level, the optelectronic properties of the phosphorescent polymers have been effectively optimized to furnish highly efficient red solution-processed PHOLEDs with a η_L of 8.31 cd A^{-1}, η_{ext} of 16.07%, and η_P of 2.95 lm W^{-1}. The present work presents valuable information to construct highly efficient red phosphorescent polymers to enhance the competence of the polymeric emitters in the field of OLEDs.

Supporting Information

Supporting Information is available from the Wiley Online Library or from the author.

Acknowledgements: J. Zhao and M. Lian contributed equally to this work. This work was financially supported by Tengfei Project from Xi'an Jiaotong University, the Fundamental Research Funds for the Central Universities, The Program for New Century Excellent Talents in University, the Ministry of Education of China (NECT-09–0651), the Key Creative Scientific Research Team in Shaanxi Province (2013KCT-05), the China Postdoctoral Science Foundation (Grant no. 20130201110034), and the National Natural Science Foundation of China (no. 20902072).

Received: August 30, 2014; Revised: September 28, 2014; Published online: November 18, 2014; DOI: 10.1002/marc.201400490

Keywords: ambipolar; aromatic silanes; functional Ir^{III} complexes; organic light-emitting diodes (OLEDs); phosphorescent polymers

[1] J. H. Burroughes, D. D. C. Bradley, A. R. Brown, R. N. Marks, K. Mackay, R. H. Friend, P. L. Burns, A. B. Holmes, *Nature* **1990**, *347*, 539.
[2] G. Gustafsson, Y. Cao, G. M. Treacy, F. Klavetter, N. Colaneri, A. J. Heeger, *Nature* **1992**, *357*, 477.
[3] a) H. Wu, L. Ying, W. Yang, Y. Cao, *Chem. Soc. Rev.* **2009**, *38*, 3391; b) G. M. Farinola, R. Ragni, *Chem. Soc. Rev.* **2011**, *40*, 3467; c) S. Gong, C. Yang, J. Qin, *Chem. Soc. Rev.* **2012**, *41*, 4797; d) X. Yang, G. Zhou, W.-Y. Wong, *J. Mater. Chem. C* **2014**, *2*, 1760.
[4] a) T.-F. Guo, S.-C. Chang, Y. Yang, R. C. Kwong, M. E. Thompson, *Org. Electron.* **2000**, *1*, 15; b) W. Zhu, Y. Mo, M. Yuan, W. Yang, Y. Cao, *Appl. Phys. Lett.* **2002**, *80*, 2045.
[5] a) J. Liu, S. Shao, L. Chen, Z. Xie, Y. Cheng, Y. Geng, L. Wang, X. Jing, F. Wang, *Adv. Mater.* **2007**, *19*, 1859; b) J. Liu, Y. Cheng, Z. Xie, Y. Geng, L. Wang, X. Jing, F. Wang, *Adv. Mater.* **2008**, *20*, 1357; c) G. Tu, C. Mei, Q. Zhou, Y. Cheng, Y. Geng, L. Wang, D. Ma, X. Jing, F. Wang, *Adv. Funct. Mater.* **2006**, *16*, 101.
[6] a) J. Jiang, C. Jiang, W. Yang, H. Zhen, F. Huang, Y. Cao, *Macromolecules* **2005**, *28*, 4072; b) X.-H. Yang, F.-I. Wu, D. Neher, C.-H. Chien, C.-F. Shu, *Chem. Mater.* **2008**, *20*, 1629; c) T. Fei, G. Cheng, D. Hu, W. Dong, P. Lu, Y. Ma, *J. Polym. Sci., A: Polym. Chem.* **2010**, *48*, 1859.
[7] a) Q. Chen, N. Liu, L. Ying, W. Yang, H. Wu, W. Xu, Y. Cao, *Polymer* **2009**, *50*, 1430; b) K. Zhang, Z. Chen, C. Yang, Y. Tao, Y. Zou, J. Qin, Y. Cao, *J. Mater. Chem.* **2008**, *18*, 291; c) K. Zhang, Z. Chen, C. Yang, Y. Zou, S. L. Gong, J. Qin, Y. Cao, *J. Phys. Chem. C* **2008**, *112*, 3907; d) W. Zhang, H. Jin, F. Zhou, Z. Shen, D. Zou, X. Fan, *J. Polym. Sci. A: Polym. Chem.* **2012**, *50*, 3895; e) J. Yu, Y. Wang, Y. Liu, X. Deng, H. Tan, Z. Zhang, M. Zhu, W. Zhu, *J. Organomet. Chem.* **2014**, *761*, 51; f) G. L. Schulz, X. Chen, S.-A. Chen, S. Holdcroft, *Macromolecules* **2006**, *39*, 9157; g) K. Zhang, Z. Chen, C. Yang, S. Gong, J. Qin, Y. Cao, *Macromol. Rapid Commun.* **2006**, *27*, 1926; h) K. Zhang, Z. Chen, Y. Zou, C. Yang, J. Qin, Y. Cao, *Organometallics* **2007**, *26*, 3699.
[8] a) Z. Ma, J. Ding, Y. Cheng, Z. Xie, L. Wang, X. Jing, F. Wang, *Polymer* **2011**, *52*, 2189; b) A. Liang, S. Dong, K. Zhang, X. Xiao, F. Huang, X.-H. Zhu, Yong Cao, *Macromol. Rapid Commun.* **2013**, *34*, 1301; c) N. R. Evans, L. S. Devi, C. S. K. Mak, S. E. Watkins, S. I. Pascu, A. Koehler, R. H. Friend, C. K. Williams, A. B. Holmes, *J. Am. Chem. Soc.* **2006**, *128*, 6647.
[9] a) J. H. Park, T.-W. Koh, J. Chung, S. H. Park, M. Eo, Y. Do, S. Yoo, M. H. Lee, *Macromolecules* **2013**, *46*, 674; b) W.-Y. Lai, J. W. Levell, M. N. Balfour, P. L. Burn, S.-C. Lo, I. D. W. Samuel, *Polym. Chem.* **2012**, *3*, 734.
[10] a) F. I. Wu, X. H. Yang, D. Neher, R. Dodda, Y. H. Tseng, C. F. Shu, *Adv. Funct. Mater.* **2007**, *17*, 1085; b) C. H. Chien, S. F. Liao, C. H. Wu, C. F. Shu, S. Y. Chang, Y. Chi, P. T. Chou, C. H. Lai, *Adv. Funct. Mater.* **2008**, *18*, 1430.
[11] a) S. Shao, J. Ding, L. Wang, X. Jing, F. Wang, *J. Am. Chem. Soc.* **2012**, *134*, 15189; b) S. Shao, J. Ding, L. Wang, X. Jing, F. Wang, *J. Am. Chem. Soc.* **2012**, *134*, 20290.
[12] Z. Ma, L. Chen, J. Ding, L. Wang, X. Jing, F. Wang, *Adv. Mater.* **2011**, *23*, 3726.
[13] a) G.-J. Zhou, C.-L. Ho, W.-Y. Wong, Q. Wang, D. Ma, L. Wang, Z. Lin, T. B. Marder, A. Beeby, *Adv. Funct. Mater.* **2008**, *18*, 499; b) W.-Y. Wong, G.-J. Zhou, X.-M. Yu, H.-S. Kwok, B.-Z. Tang, *Adv. Funct. Mater.* **2006**, *16*, 838; c) G. Zhou, W.-Y. Wong, B. Yao, Z. Xie, L. Wang, *Angew. Chem. Int. Ed.* **2007**, *46*, 1149; d) X. Xu, X. Yang, J. Dang, G. Zhou, Y. Wu, H. Li, W.-Y. Wong, *Chem. Commun.* **2014**, *50*, 2473.
[14] a) Y. T. Tao, Q. Wang, C. L. Yang, Q. Wang, Z. Q. Zhang, T. T. Zou, J. G. Qin, D. G. Ma, *Angew. Chem. Int. Ed.* **2008**, *47*, 8104; b) Y. T. Tao, C. L. Yang, J. G. Qin, *Chem. Soc. Rev.* **2011**, *40*, 2943.
[15] Y. Tao, Q. Wang, L. Ao, C. Zhong, J. Qin, C. Yang, D. Ma, *J. Mater. Chem.* **2010**, *20*, 1759.
[16] S. Aoki, Y. Matsuo, S. Ogura, H. Ohwada, Y. Hisamatsu, S. Moromizato, M. Shiro, M. Kitamura, *Inorg. Chem.* **2011**, *50*, 806.
[17] K. Zhang, Z. Chen, Y. Zou, S. Gong, C. Yang, J. Qin, Y. Cao, *Chem. Mater.* **2009**, *21*, 3306.